Electron and hole in-plane g-factors in single InAs quantum rings

2015 J. Phys.: Conf. Ser. 647 012011

(http://iopscience.iop.org/1742-6596/647/1/012011)

Journal of Physics: Conference Series **647** (2015) 012011 doi:10.1088/1742-6596/647/1/012011

Electron and hole in-plane g-factors in single InAs quantum rings

R. Kaji[1], T. Tominaga[1], Y.-N. Wu[2], S.-J. Cheng[2], and S. Adachi[1]

[1] Department of Applied Physics, Hokkaido University, Sapporo, Japan
[2] Department of Electrophysics, National Chiao Tung University, Hsinchu, Taiwan

E-mail: r-kaji@eng.hokudai.ac.jp

Abstract. The electron and hole in-plane g-factors were studied in individual InAs/GaAs quantum rings (QRs). From the magneto-photoluminescence measurements under a transverse magnetic field, we evaluated the in-plane g-factors of electron and hole spins by rotating the sample systematically along the crystal growth axis. The experimental results indicate that the in-plane and the out-of-plane anisotropies in hole g-factor are larger than those of electron g-factor, and the value of the hole in-plane g-factor varies largely from QR to QR while the electron g-factor is almost a constant value. From the model calculation considering the effects of shape anisotropies and uniaxial stress, we examined the correlation between the in-plane g-factors and the degree of valence band mixing. Further, the experimentally obtained trend in g-factors was in agreement qualitatively with theoretical consideration.

1. Introduction

Spin confined in the semiconductor nanostructures is one of the prospective candidates for the basis in coming quantum information technology. The confinement of carrier wave functions yields a long spin coherence time via the strong suppression of spin relaxation processes originated from the spin-orbit interaction, and indeed, quite longer spin coherence times compared to that reported in the bulk or quantum wells have been achieved in the quantum dots (QDs). [1] Thus, the spin manipulation in these systems has gained considerable attention from both scientific and engineering viewpoints. Since the hole spin is expected to have a longer coherence time than the electron spin in QDs due to a weaker interaction with lattice nuclei, [2, 3] an arbitrary manipulation of hole spin is especially favored.

One of the key parameters for spin manipulation is carrier g-factor. Several works have focused on developing techniques for the control and the evaluation of electron and/or hole g-factors. These techniques include the appropriate adoption of materials and structures in III-V bulk semiconductors, [4] the application of bias voltages to In(Ga)As QDs, [5, 6] and the utilization of nuclear spin polarization in InAlAs QDs. [7] Since In(Ga)As and GaAs are widely-used III-V materials, the electron and hole g-factors in their QDs have been studied intensively. [8]

In this study, we focus on the electron and hole g-factors (g^e, g^h) in the individual InAs/GaAs quantum rings (QRs). Semiconductor QRs exhibit not only the discrete energy levels like QDs, but also the distinctive properties such as the Aharanov-Bohm effect. [9, 10] In the previous work, we have evaluated the longitudinal components of (g^e, g^h), where the hole g-factor showed the correlation to the degree of valence band mixing. [11] In order to obtain the comprehensive knowledge of g-factors in QRs, we investigated the transverse components of (g^e, g^h) in the same InAs/GaAs QR sample.

2. Sample and Setup

A self-assembled InAs/GaAs QR sample grown on an undoped (100) GaAs substrate [12] was studied under the transverse magnetic fields ($|B_\perp| \leq 5$ T) at 6 K. The average inner and outer radii and height of QR were found to be 10 nm, 40 nm, and 1.5 nm, respectively, from AFM measurements on a reference uncapped layer. These values were considered in the model calculations described below. Photoluminescence (PL) spectra from single QRs were detected by a triple grating spectrometer and a liquid N_2-cooled Si-CCD. The energy resolution to determine the spectral peaks was $\sim$5 μeV. A cw-Ti:sapphire laser tuned to the transition energy at the wetting layer of QRs ($\lambda \sim$864 nm) was employed for excitation, and its polarization was set to temporal averaging nonpolarization in order to avoid the additional effects depending on the initial population of carrier spins. [13] The polarization of PL signal was determined by a rotating half-wave plate and a linear polarizer inserted in the detection path.

3. Results and Discussion

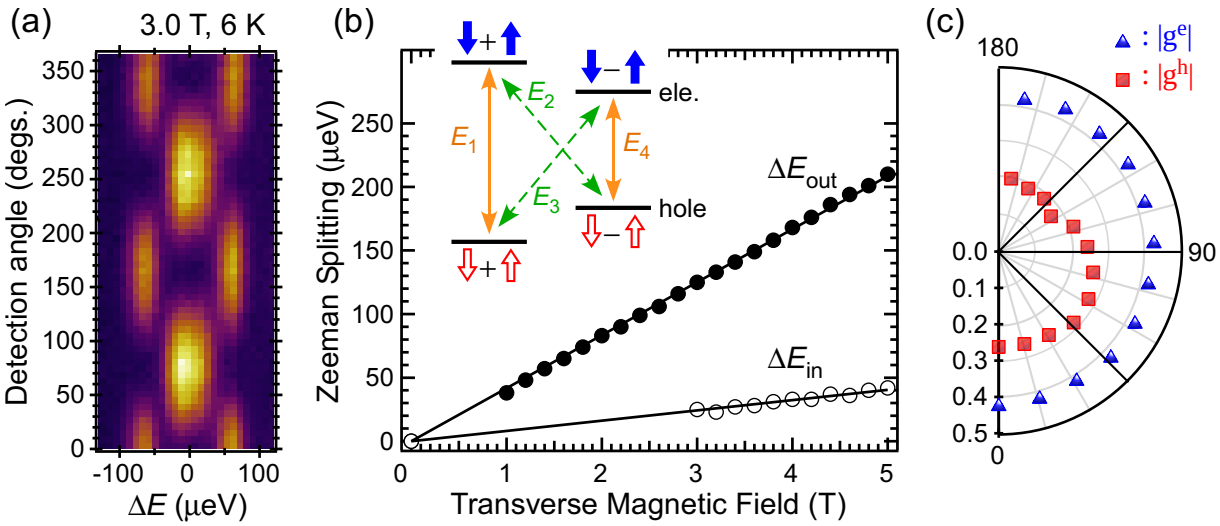

Figure 1. (a) 2D plot of the charged exciton PL as a function of the detection angle. The horizontal axis was converted to the energy difference (ΔE) from E_0(=1.3272 eV). (b) Energy splittings of the outer and inner peaks as a function of $B_\perp$. Inset shows the energy diagram of electron (hole) spins depicted as solid (open) arrows. (c) Polar plot of $|g^e_\perp|$ (triangles) and $|g^h_\perp|$ (squares) in a typical individual QR.

First, we explain briefly the evaluation of the electron and hole in-plane g-factors ($g^e_\perp$, $g^h_\perp$). As shown in the inset of Fig. 1(b), the transverse magnetic field $B_\perp$ induces the spin-state mixing, and thus, the four transitions (E_1, E_2, E_3, E_4) with linearly polarized emission and absorption become optically-active. The magnitudes of ($g^e_\perp$, $g^h_\perp$) can be deduced from the Zeeman splittings of the outer peaks $\Delta E_{\rm out}$=$E_1 - E_4$ and the inner peaks $\Delta E_{\rm in}$=$E_2 - E_3$ whose proportional coefficients are given by the sum or difference of ($|g^e_\perp|$, $|g^h_\perp|$). Figure 1(a) shows the PL spectra of the charged exciton from a typical single QR as a function of the detection angle under $B_\perp$=3.0 T. The spectra indicate the four peaks with cross-linear polarizations between the outer (E_1, E_4) and inner peaks (E_2, E_3), and the Zeeman splitting $\Delta E_{\rm out}$ ($\Delta E_{\rm in}$) depicted as solid (open) circles in Fig. 1(b) increases linearly with increasing $B_\perp$. From the line fittings, the in-plane g-factors were found to be $|g^e_\perp|$=0.43 $\pm$ 0.01 and $|g^h_\perp|$=0.26 $\pm$ 0.01.

Further, we investigated the in-plane anisotropies of ($|g^e_\perp|$, $|g^h_\perp|$) by rotating the sample around the crystal growth axis (z-axis). Figure 1(c) shows the polar plot of ($|g^e_\perp|$, $|g^h_\perp|$). While $|g^e_\perp|$ (triangles) shows the isotropic nature, $|g^h_\perp|$ (squares) varies depending on the direction of $B_\perp$ and shows the anisotropic feature. To quantify the degree of anisotropy in ($|g^e_\perp|$, $|g^h_\perp|$), we introduced an anisotropic parameter $\alpha^i = (|g^i_{\rm max}| - |g^i_{\rm min}|)/|\overline{g^i_\perp}|$ (i= e, h), where $|g^i_{\rm max(min)}|$ is the maximum (minimum) value of $|g^i_\perp|$ and

$|\overline{g_\perp^i}|$ is the average value over the measurements under the different direction of $B_\perp$. The anisotropic parameters of ($|g_\perp^e|$, $|g_\perp^h|$) in this QR were found to be $\alpha^e = 0.035$ and $\alpha^h = 0.470$, respectively.

We performed the same procedure for the several QRs in the same sample and obtained the following findings; $|\overline{g_\perp^h}|$ varies largely from QR to QR ($0.04 \leq |\overline{g_\perp^h}| \leq 1.03$) compared to $|\overline{g_\perp^e}|$ ($0.34 \leq |\overline{g_\perp^e}| \leq 0.50$), and α^h is larger than α^e for most of the measured QRs. In addition, g^h shows a large out-of-plane anisotropy, that is, a large difference between the transverse and the longitudinal components ($|\overline{g_\perp^h}|_{ave} = 0.58$, $|g_\parallel^h|_{ave} = 1.50$) as contrast with the small out-of-plane anisotropy of g^e ($|\overline{g_\perp^e}|_{ave} = 0.44$, $|g_\parallel^e|_{ave} = 0.60$). [11] The observed differences in (g^e, g^h) are attributed to the differences in the symmetry of their Bloch functions and/or in the mixing with the other energy bands.

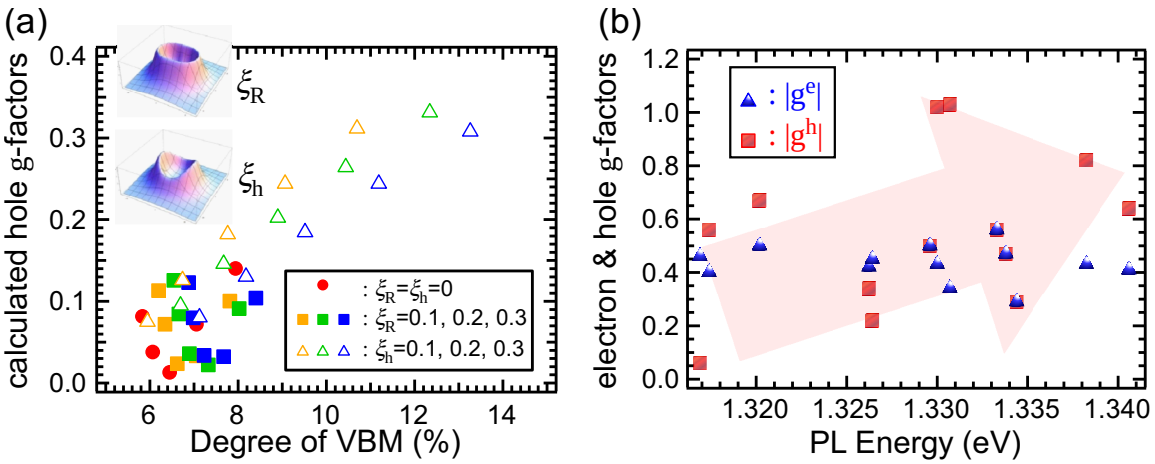

Figure 2. (a) The calculated hole g-factors in x-direction as a function of β. Various symbols indicate the implementation of the shape anisotropies in height and radius (ξ_h, ξ_R) and the external stress in x-direction. The QR size was fixed to the measured mean size. (b) Experimentally obtained $|g_\perp^e|$ (triangles) and $|g_\perp^h|$ (squares) as a function of E_{PL} of the corresponding individual QRs. $|g_\perp^h|$ indicates a certain degree of dependence on E_{PL} while $|g_\perp^e|$ is in almost constant over the whole range.

Next, we consider the effect of band mixing, especially in the valence band mixing (VBM), on the observed ($|g_\perp^e|$, $|g_\perp^h|$). The VBM, which is the band mixing between the heavy holes (HHs: $\varphi_{\pm 3/2}$) and the light holes (LHs: $\varphi_{\pm 1/2}$), changes the pure HHs to the "*mainly HHs*" defined as $|\tilde{\varphi}^\pm\rangle = (|\varphi_{\pm 3/2}\rangle + |\beta| e^{\pm i 2\theta_s} |\varphi_{\mp 1/2}\rangle)/\sqrt{1+\beta^2}$, where β and θ_s are the degree of VBM and the coupling phase, respectively. One of the remarkable effects originated from VBM is the modulation of g^h, which has been reported for the longitudinal component. [11] The in-plane g-factors of pure HHs and LHs can be written as $g_\perp^{HH} = 3q_\perp$ and $g_\perp^{LH} = 4\kappa_\perp + 10q_\perp$, respectively ($q_\perp$, $\kappa_\perp$: in-plane component of Luttinger parameter). Although $g_\perp^{HH}$ in bulk semiconductor is negligible due to the relation $q_\perp \ll \kappa_\perp$, non-zero values of hole in-plane g-factors have been observed commonly in the self-assembled QDs and QRs. The reason is that the VBM is enhanced in these self-assembled structures, and thus, the state we could access is not the pure HH but the *mainly HH*. In general, the origin of the VBM is attributed to the confinement of carrier spins and the anisotropies in the shape, in the interfacial properties, [14] and in the distribution of the residual strain. [15] Since our QRs were originated from self-assembled QDs formed with the lattice mismatch to the barrier component, the residual strain was the most expected source of VBM. Note that the VBM does not affect so much on g^e even in the QDs and QRs.

Figure 2(a) shows the calculated hole g-factor in x-direction (g_x^h) as a function of the degree of VBM, β, for asymmetric strained QRs. The simulation was carried out using Luttinger-Kohn four band $\boldsymbol{k}\cdot\boldsymbol{p}$ theory [16] for volcano-shaped QRs with the consideration of shape anisotropies in height and radius of ring (parametrized by the parameters ξ_h and ξ_R, respectively). [17] To highlight the VBM effects, a

controlled external uniaxial stress was applied to the QRs along the shape-elongation axis, and it was varied from $\sigma = -0.2$ GPa (compressive) to $\sigma = +0.2$ GPa (tensile) to tune the degree of VBM and to examine the corresponding changes of g-factor, as shown in Fig. 2(a). Other parameters used in the calculation were adopted by considering the materials of QR and barrier layers. From the calculation, the following was found; increasing the shape anisotropies ($\xi_{\rm h}$, $\xi_{\rm R}$) and the magnitude of the tensile stress, the degree of VBM and resultant $\mathrm{g}_x^{\rm h}$ increase as overall trend since they enhance the anisotropy in the system of our model. Although the magnitude of calculated $\mathrm{g}_x^{\rm h}$ are smaller than the experimentally obtained $|\mathrm{g}_\perp^{\rm h}|$ at this stage, all calculated points agree with simple consideration. Further, we found that even without the effects of shape anisotropies and the external stress, the quantum confinement could induce a significant VBM about 6.5% in our small QRs.

To confirm the theoretical considerations, we plotted the observed g-factors ($|\mathrm{g}_\perp^{\rm e}|$, $|\mathrm{g}_\perp^{\rm h}|$) as a function of the PL energy ($E_{\rm PL}$) in Fig. 2(b). $E_{\rm PL}$ can be used as a measure of the confinement strength of carrier wave functions. Although the large variation in a whole range of $E_{\rm PL}$ obscures the trend, $|\mathrm{g}_\perp^{\rm h}|$ seems to increase with increasing $E_{\rm PL}$, and this point is in contrast with the case of $|\mathrm{g}_\perp^{\rm e}|$; it seems to keep a constant value. The increase in the confinement strength yields the increases in both $E_{\rm PL}$ and β. Thus $|\mathrm{g}_\perp^{\rm h}|$ is expected to increase corresponding to the change in $E_{\rm PL}$, and indeed, this simple consideration agrees qualitatively with experimental observation. More detailed discussion including the quantitative comparison between experimental and theoretical results will been seen in future works.

4. Conclusion

The electron and hole in-plane g-factors in individual self-assembled InAs/GaAs QRs were studied. The evaluated hole in-plane g-factor varies largely from QR to QR, and the in-plane and the out-of-plane anisotropies in hole g-factor were observed; these features were contrast with the case of electron g-factor. From the model calculation, the effects of in-plane anisotropies and the confinement of carrier spins on the degree of VBM and the resultant change in hole in-plane g-factor were investigated. Although more detailed discussions are necessary for the quantitative agreement between the experimental and theoretical results, our observations will serve a useful information for the hole spin manipulation in nanostructures.

Acknowledgments

We are grateful to S. Suraprapapich and C. W. Tu of the University of California, San Diego, for providing the quantum ring samples. This work has been supported by JSPS KAKENHI Grant Number 26800162.

References

[1] Greilich A, Oulton R, Zhukov E A, Yugova I A, Yakovlev D R, Bayer M, Shabaev A, Efros Al L, Merkulov I A, Stavarache V, Reuter D and Wieck A 2006 *Phys. Rev. Lett.* **96**, 227401
[2] Testelin C, Bernardot F, Eble B and Chamarro M 2009 *Phys. Rev.* B **79**, 195440
[3] Kaji R, Ohno S, Hozumi T and Adachi S 2013 *J. Appl. Phys.* **113** 203511
[4] Kosaka H, Kiselev A A, Baron F A, Kim K W and Yablonovitch E 2001 *Electron. Lett.* **37** 464
[5] Nakaoka T, Tarucha S and Arakawa Y 2007 *Phys. Rev.* B **76** 041301(R)
[6] Bennett A J, Pooley M A, Cao Y, Sköld N, Farrer I, Ritchie D A and Shields A J 2013 *Nat. Comm.* **4** 1522
[7] Kaji R, Adachi S, Sasakura H and Muto S 2007 *Appl. Phys. Lett.* **91** 261904
[8] Bayer M, Kuther A, Forchel A, Gorbunov A, Timofeev V B, Schafer F and Reithmaier J P 1999 *Phys. Rev. Lett.* **82** 1748
[9] Lorke A, Luyken R J, Govorov A O and Kotthaus J P 2000 *Phys. Rev. Lett.* **84** 2223
[10] Bayer M, Korkusinski M, Hawrylak P, Gutbrod T, Michel M and Forchel A 2003 *Phys. Rev. Lett.* **90** 186801
[11] Kaji R, Hozumi T, Hachiyama Y, Tomii T, Sasakura H, Jo M and Adachi S 2014 *Appl. Phys. Express* **7** 065002
[12] Suraprapapich S, Panyakeow S and Tu C W 2007 *Appl. Phys. Lett.* **90** 183112
[13] Ohno S, Adachi S, Kaji R, Muto S and Sasakura H 2011 *Appl. Phys. Lett.* **98** 161912
[14] Krebs O and Voisin P 1996 *Phys. Rev. Lett.* **77** 1829
[15] Léger Y, Besombes L, Maingault L and Naruette H 2007 *Phys. Rev.* B **76** 045331
[16] van Bree J, Silov A Yu, Koenraad P M, Flatté M E and Pryor C E 2012 *Phys. Rev.* B **85** 165323
[17] Fomin V M, Gladilin V N, Klimin S N, Devreese J T, Kleemans N A J M and Koenraad P M, 2007 *Phys. Rev.* B **76** 235320